FE analysis of 6063 aluminium profiles with complex cross-section during online quenching processes

R. B. Mei*,**, L. Bao**, C. S. Li*, J.K. Wang**, X. H. Liu*
*State Key Laboratory of Rolling and Automation, Northeastern University, Wenhua Str. 3, 100819 Shenyang, China
**Northeastern University at Qinhuangdao, Northeastern University, Taishan Str.143, 066004 Qinhuangdao, China,
Email: meirb1999@gmail.com

1. Introduction

Aluminum alloys of the 6063 type (Al-Mg-Si) have some advantageous properties that make them an excellent structural material choice for a number of applications in aerospace and construction [1]. The mechanical properties are improved by controlling the second phase precipitation, and 6××× alloys can be aged if cooling is performed at a proper cooling rate [2]. Gbenebor, et al. [3] studied the influence of water and air cooling coupled with inoculation on the mechanical properties of 6063 aluminum alloy through adding into Ni powder particles. The quench sensitivity of 6063 alloy has been investigated via constructing TTP curves and the critical temperature ranges from 300°C to 400°C with the nose temperature of about 360°C [4].

Aluminum extrusion is capable of producing long solid or hollow sections with very complex cross-section geometries. Cooling immediately after extrusion is critical for the nucleation of the high densities of strengthening particles in alloys, such as AlMgSi [2]. Because the hot extrusion temperature is high enough to keep Mg and Si to remain in solution before cooling, it is efficient to use an online cooling to room temperature followed by aging in order to obtain the full potential strength [5]. In spite of the water cooling or forced air cooling is generally used to rapid cooling, no medium is better than water especially because it is both cheap and easy. However, it is difficult to avoid the distortion and high residual stresses across the section and length due to variations in thickness and non-uniform cooling during online quenching process. In order to describe the shape distortion due to non-uniform cooling, a rectangular plate and a simple section with two different thicknesses are used to investigate the distortion with water cooling from the top side and air cooling from the bottom side and different initial cooling rate [2,6-7]. The width ratio has a varying effect on the distortion, while the non-uniformity ratio and the thickness and width of the section have an almost consistent effect. Furthermore, the method to reduce the residual stress and distortion in quenching process are investigated by some researchers [8-9] and the cold stretching and cyclic load has significant effect on the reduction of residual stress [10-12].

Appropriate modeling, using both physical and numerical methods is efficient to achieve a better cooling strategy. Nallathambi et al. [13] worked on mathematically formulating quenching process by means of a nonlinear finite element technique which included the coupling of thermal, metallurgical and mechanical fields. An enhanced quenching at the mass lumped regions and with a reduced quenching at the edges and corners, stresses and distortion can be minimized simultaneously. A complex thermo-mechanical model formulated on the basis of J2-plasticity theory to simulate the quenching process of steel profiles is studied and the validity of the model is verified by comparing the simulation results with experimental measurements [14]. Zabaras et al. [15] presents a FE procedure on the basis of solution of heat transfer and inelastic problems for calculation of temperature and stresses during cylinders quenching processes. Carlone et al. [16-17] developed a computational thermo-metallographic and thermal elasto-plastic model to evaluate the transient stress, strain distributions and the final phases and hardness distributions on the basis of JMAK model. A lot of researchers have also used FE software such as ABAQUS [2, 6, 8], FLUENT [9] to simulate and analyze the distortion and residual stress simple cross-section profiles such as plate with different thickness and bar during the online quenching process. As the commercial finite-element software, ANSYS has been used to analyze and optimize the quenching process without considering of the movement of workpiece [18-19].

In the present work, the 3D finite element method based on ANSYS is developed and used to simulate the online quenching processes. Firstly, the experiments and calculation for the temperature and displacement of a plate were carried out to verify the developed model. In addition, the program of heat transfer coefficient (HTC) at any time was developed and embedded into ANSYS in order to realize the movement of profile during online quenching. Then the temperature, stress and displacement of an actual complex cross-section profile from one plant in online quenching processes were investigated according to the simulated results. Finally, the influence of external stretching force on the reduction of distortion of profile was also investigated using simulation.

2. FE modeling

The material considered in this study was the 6063 alloy. The physical and mechanical properties are actually temperature dependent, but they were assumed to be constant except expansion coefficient in this study. The physical and mechanical properties [20] are following as: density is 2700 kg/m^3, conductivity is 2018 W/mK, specific heat is 900 J/kg°C, elastic modulus is 7000 MPa, Yield stress is 48 MPa, tangent modulus is 16.1 MPa and Poisson ratio is 0.33. Furthermore, the expansion coefficient is 2.18e-5, 2.34e-5, 2.45e-5, 2.56e-5 and 2.67e-5 (1/°C) with

20, 100, 200, 300 and 400°C, respectively.

The parameters used to simulate water cooling process and the sizes of profile cross-section are shown in Fig. 1, a. There are two cooling conditions including air cooling from exit position to quenching region and water cooling during online quenching of profiles. The length of air before quenching and water cooling region is set to 300 m and 600 mm, respectively, according to the design of quenching line. The influence of extrusion process on the stress and distortions is ignored so that the stress and distortion before quenching is assumed as zero in the study. The temperature of profile at exit position is set as the uniform 490°C. Both the water and ambient temperature is set to 20°C, and the extrusion speed is 0.05 m/s. The mesh size had been considered of reducing large computational time and making reliable predictions so that three to four elements were used across the thickness (Fig. 1, b) in this study. There are total 243789 elements and 298587 nodes in the meshed model.
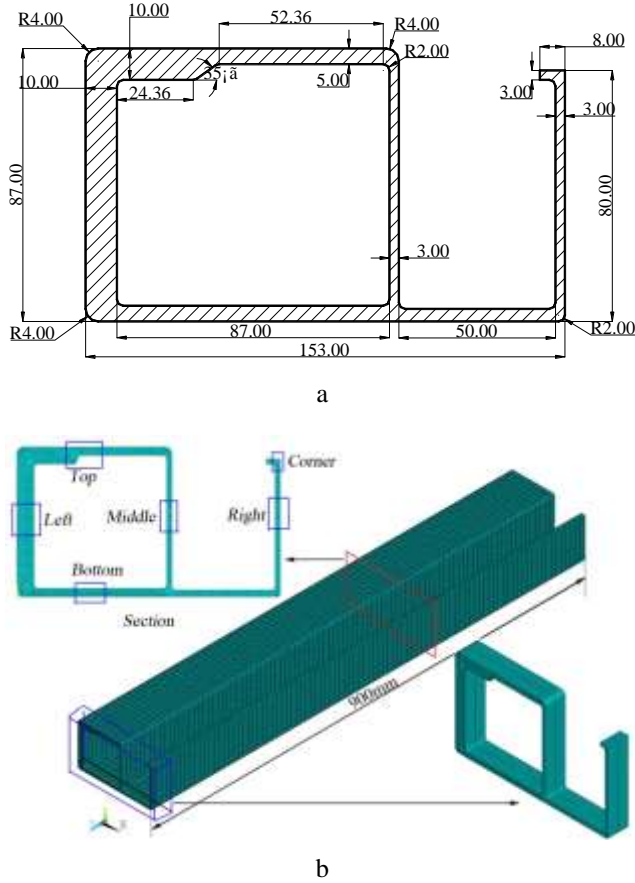

Fig. 1 Geometry size and mesh model: a - geometry section size; b - schematic of mesh model

The 3D FE simulations were performed with the ANSYS software. The brick element 70 and 45 for thermal and structure analysis, respectively, were chosen to analyze coupled thermal-stress field. The transient temperature field T in the profiles is assumed to depend on the coordinate x, y, z and time t [21].

$$k\left(\frac{\partial^2 T}{\partial x^2} + \frac{\partial^2 T}{\partial y^2} + \frac{\partial^2 T}{\partial z^2}\right) + \dot{q} - \rho c \frac{\partial T}{\partial t} = 0, \qquad (1)$$

where T is the transient temperature of infinitesimal body,

K; ρ is the material density, kg/m³; c is the material specific heat, J/kg K; k is the material heat conductivity, W/(m K); t is the time, s; $\dot{q}$ is the inner heat resource, J/m³.

The cooling intensity is characterized by the heat transfer coefficient (HTC). The HTC is highly temperature dependent and its variations are generally classified into four different regimes including film boiling, transition boiling, nucleate boiling and natural convection [6]. In the study, the HTC for water cooling is described as follows:

$$h_c = \begin{cases} 62.5 T_w & T_w \leq 160^{\circ}C \\ -50 T_w + 18000 & 160^{\circ}C < T_w \leq 320^{\circ}C \\ -\frac{25}{8} T_w + 3000 & 320^{\circ}C < T_w \leq 600^{\circ}C \end{cases}, \qquad (2)$$

where h_c is heat transfer coefficient, W/(m² K); T_w is the surface temperature of profiles, °C.

For coupled thermal-structure analysis, higher stress occurred because of larger temperature change, which perhaps results in the plastic deformation during online quenching process. Suppose each load step is smaller, the incremental stress-strain in the elastic region is:

$$\Delta\{\sigma\} = [D]\left(\Delta\{\varepsilon\} - \Delta\{\tilde{\varepsilon}\}_T\right), \qquad (3)$$

where $[D]$ is elastic matrix, α is the linear expansion coefficient and $\Delta\{\tilde{\varepsilon}\}_T = \left[\{\alpha\} + \mathrm{d}[D]^{-1}/dT\{\sigma\}\right]^T$.

In the plastic region, the incremental-strain relation is written in [22]:

$$\Delta\{\sigma\} = [D]_{ep}\left(\Delta\{\varepsilon\} - \Delta\{\tilde{\varepsilon}\}_T\right) + \Delta\{\tilde{\sigma}\}_T, \qquad (4)$$

where $[D]_{ep}$ is elastoplastic matrix; $\Delta\{\tilde{\sigma}\}_T$ is the incremental plastic-strengthened temperature stress.

The thermal-structure model for online quenching with water and air cooling was developed in ANSYS environment which employs an iterative solver to solve temperature and displacement. During online quenching, the profile moves and heat transfer boundary changes atany position and time. Therefore, the solution of transient temperature with time and different boundary conditions was realized by developed programs. The flowchart of the coupling methodology is shown in Fig. 2.

In order to verify the FE model, the temperature and displacement of a plate during quenching is studied by numerical simulation and experiments. The experimental plate size is 1000 mm×50 mm×3 mm and the length of water cooling region is 800 mm. The experimental aluminium alloy plate come from the cross-section extrusion in the extruding machine JY-800T. The plate is heated to 490°C and then quenched in the water cooling region. The number of elements along the thickness, width and length is 4, 25 and 100, respectively (Fig. 3, a). The top surface is water cooling but the bottom surface is still air cooling. The temperature and displacement is showed in Fig. 3, b. Where, point M and N lies to the top and bottom surface of
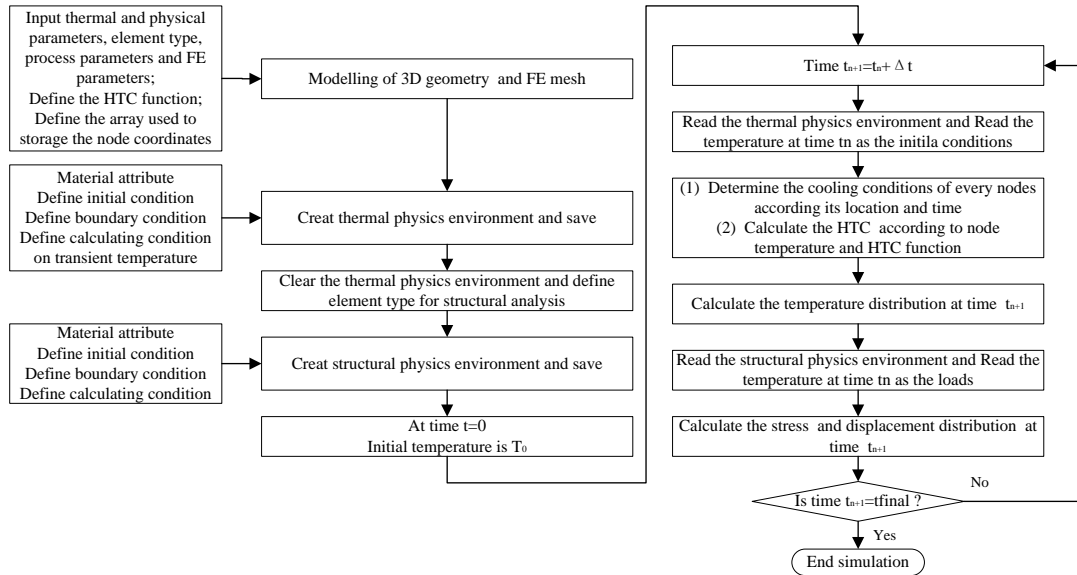
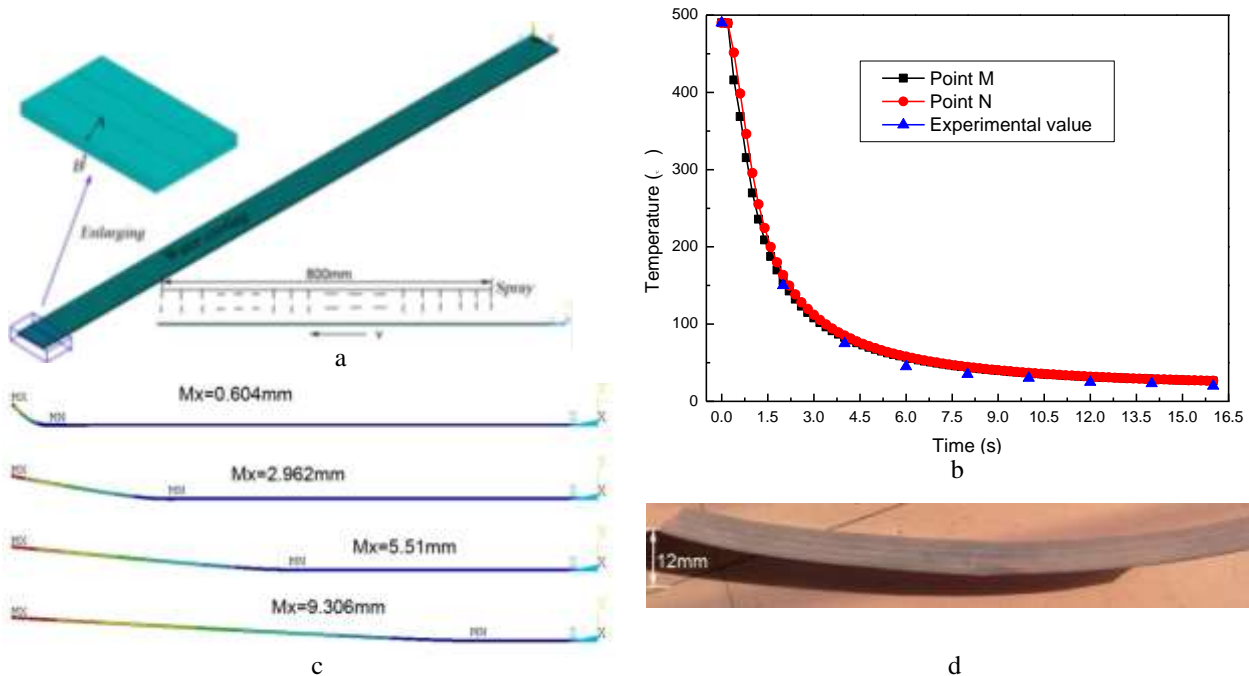Fig. 2 Flowchart of the coupling methodology

Fig. 3 Plate mesh model, temperature and final displacement: a - FE mesh; b - temperature; c - Y-component of displacement; d - experimental sample

head of plate in the simulation, respectively (Fig. 3, a). The temperature at the center of head of plate at real time and displacement in thickness direction are also measured continuously by the ST20-A05 (Fig. 3, b). Where, *Mx* and *Mn* express maximum and minimum value of calculated results such as temperature (Fig. 4), displacement (Fig. 3, c and (Fig. 6, a), stress (Fig. 6, b) and so on. With the increment of quenching length, the temperature decreases but displacement increases obviously (Fig. 3, c). The point M has the same temperature as point N due to less thickness of the plate. The calculated temperature and displacement are in good agreement with the measured value so that the FE model is reliable.

3. Results and discussion

The temperature distribution at different cooling time is shown in Fig. 4. The length of profile in quenching regions is about 100 mm at time 2 s. Because the thickness of left profiles (Fig. 1, a) is larger three times than right so that the maximum and minimum value of temperature is about 63.7°C and 347.9°C, respectively, which lies in the region of B and H points (Fig. 4, d). Furthermore, the different thickness leads to the order of temperature from high to low is left, top, bottom, middle and right. In spite of the profiles move into the quenching region, the heat transfer boundary of B point is air cooling due to lie in hollow side compared with that the A points. The temperature of inside of hollow profiles is higher than that of outside. The minimum value of temperature is 24.4℃ and 20.7℃ at time 7 and 12 s respectively. Therefore, the temperature and cooling rate is satisfied with the requirements of online quenching.
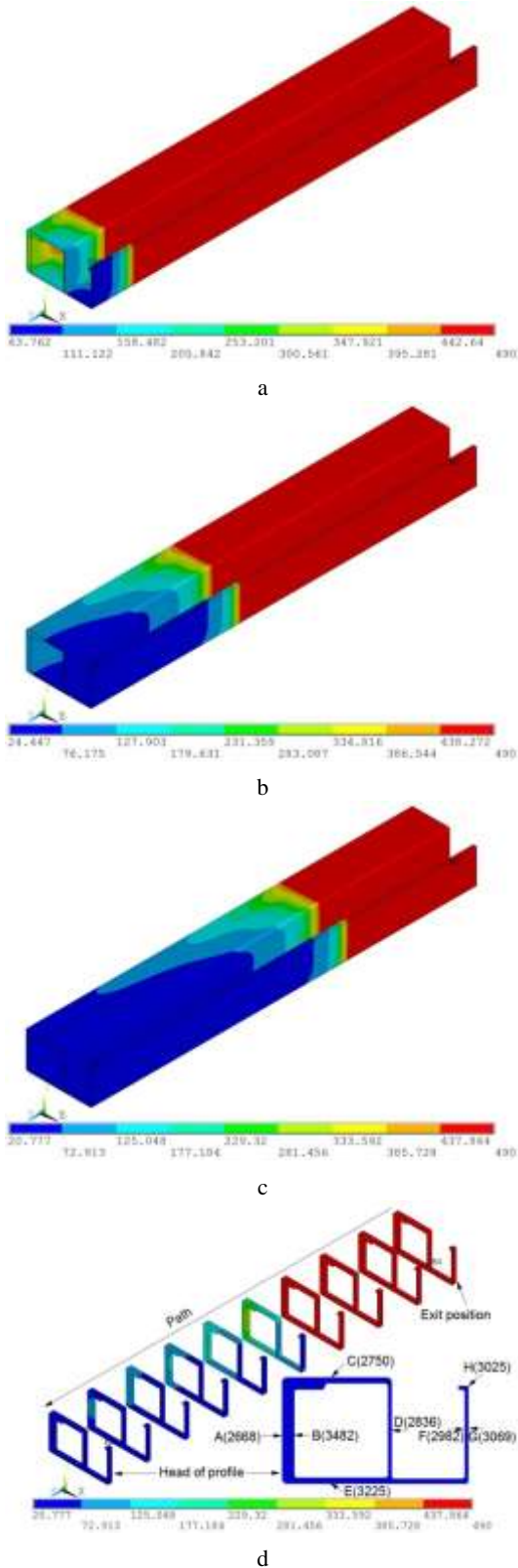
Fig. 4 Distribution of temperature with different time: a - $t = 2$ s; b - $t = 7$ s; c - $t = 12.0$ s; d - $t = 12$ s (isometric sections)

The temperature distribution along the typical paths (Fig. 4, d) is shown in Fig. 5, a. Where the path A is described by all of nodes with the same x and y coordinates as nodes A and the node A is the final position of the path. It is found that the temperature distribution across the length is divided into two regions obviously due to air and water cooling process. The temperature decreases about

10~40℃ from the exit position to quenching region. Furthermore, the temperature decreases significantly at initial water cooling stage and then the cooling rate becomes slower during online quenching process. Finally, the temperature of these typical point is cooled to about 20~80℃.
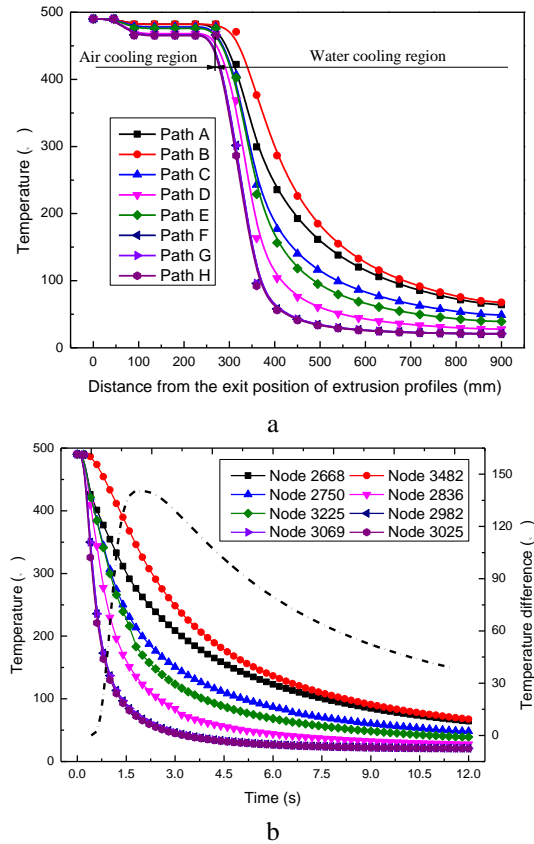

Fig. 5 Change of temperature: a - typical path; b - typical points and temperature difference

The temperature of these typical points at the head cross-section of profile decreases greatly within 3.5 s (Fig. 5, b). The points F (Node 2982), G (Node 3069) and H (Node 2668) has the maximum cooling rate 200°C/s and the temperature decreases faster than the other points. It is found obviously that the different thickness across section leads to the order cooling rate from points A, C, E, D to H. In spite of the temperature of B (Node 3482) points is higher than A (Node 2668) and the temperature difference become smaller after quenching. Furthermore, the temperature difference between the points B and H increases at first then decreases and the value is less about 40°C after quenching.

The displacement and Mises equivalent stress when the head of profile moved out of quenching region is shown in Fig. 6. It can be seen from the Fig. 6, a that non-uniform cooling rate results in distortion. Furthermore, the right side of profile has the larger deformation than left side leads to the head of profile bends obviously across the length. The maximum of total displacement is about 8 mm with length 600 mm so that the non-uniform deformation become more obviously with the increment of quenching length. All of the stress distributions are non-uniform significantly because of non-uniform deformation. In addition, the maximum Mises equivalent stress is about 57.2 MPa higher than yield stress results in plastic deformation and residual stress (Fig. 6, b).
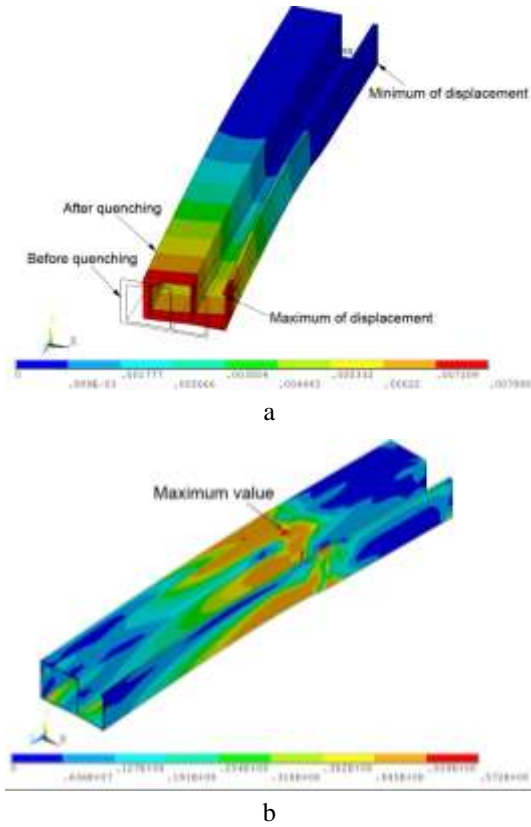
a

b

Fig. 6 Distribution of total displacements and Mises equivalent stress after quenching

The temeprature difference among three typical points A, C and H is significantly and the x-component and y-component displacement distribution along the typical path A, C, H is investigated (Fig. 7). The thickness diffe-
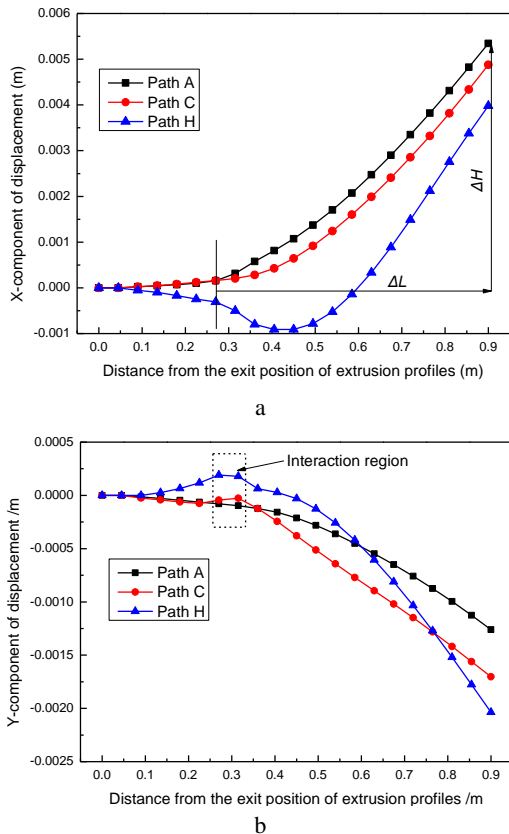

a

b

Fig. 7 Displacement along typical path: a - X-component displacement; b - Y-component displacement

rence across the width is larger than height leads to larger X-component displacement. Thickness difference leads to X-component and Y-component displacement along path C increase up to about 5.5 and 2.0 mm, respectively. However, for path H, the X-component and Y-component displacement change up to 1mm and 0.3mm (in the interaction region), and then increase to a final value 4.0 and 2.2 mm in the opposite direction. In addition, the X-component and Y-component displacement difference between points A and H increase up to a maximum value and then decrease to 2.2 and 1 mm, respectively, after quenching. According to the $\varDelta H$, m and $\varDelta L$, m, the total X-component and Y-component displacement perhaps is 100 and 30 mm, respectively, after finishing extrusion because the actual length of profiles is about 9-10 m.

Fig. 8 shows the X, Y and Z-component stress distribution across the length. It is found obviously that the stress change complicately across the length during the quenching process. The σ_x along the path A and E increases up to a maximum value about 50 MPa and then decre-
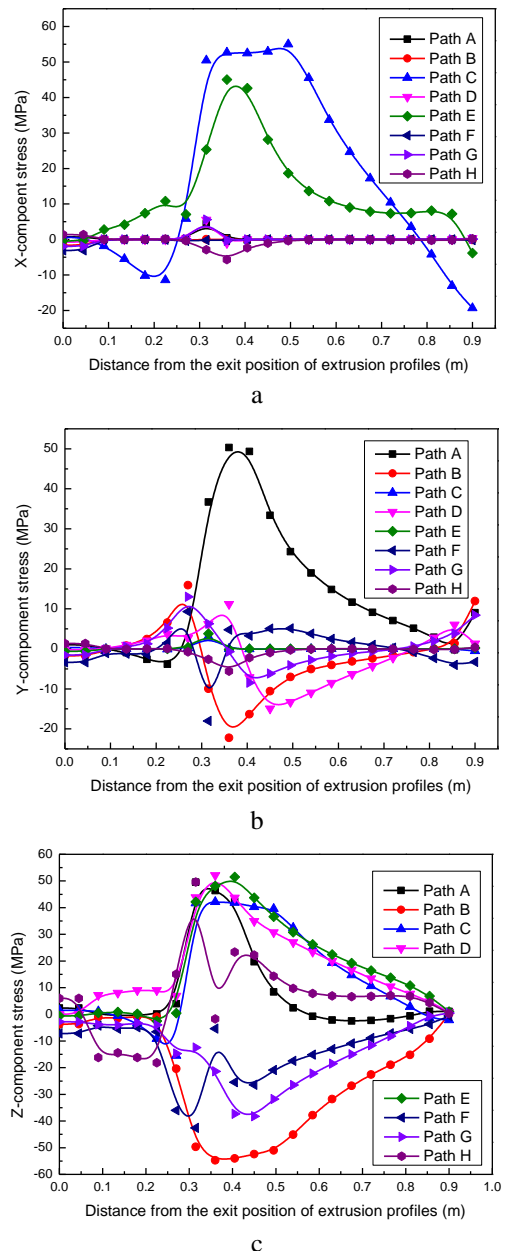

a

b

c

Fig. 8 Stress distribution across typical paths: a - X-component; b - Y-component; c - Z-component
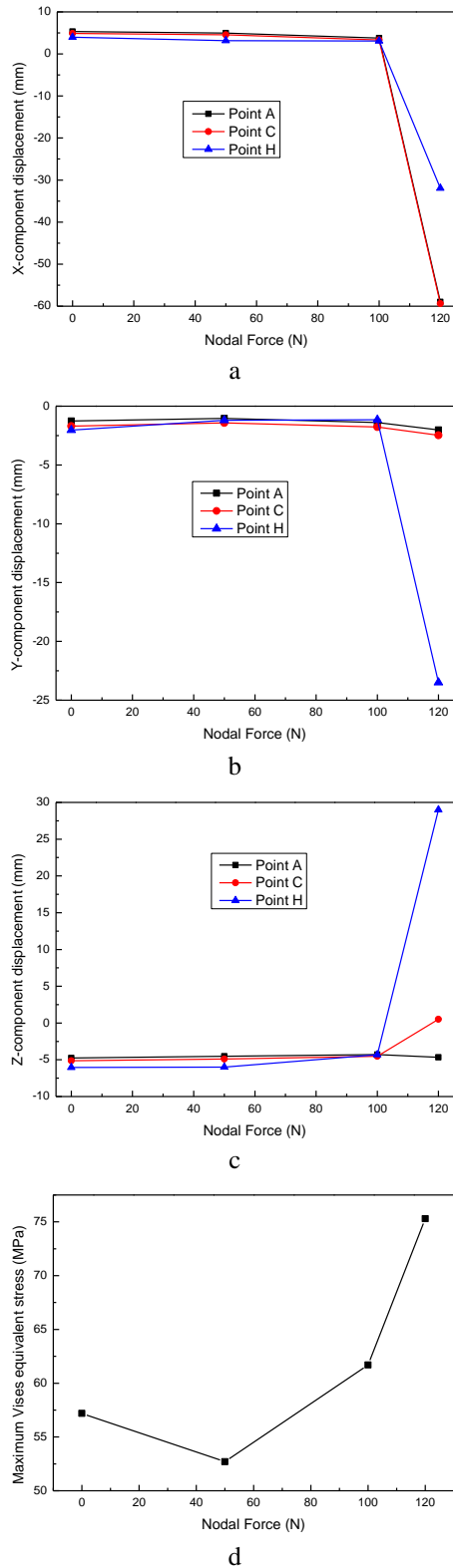
a

b

c

d

Fig. 9 Displacement and equivalent stress under different nodal force: a - X-component displacement; b - Y-component displacement; c - Z-component displacement; d - Maximum Mises equivalent stress

ase to a final value but the stress keeps unchanged along the other paths. The non-uniform deformation before and after quenching leads to the σ_y and σ_z distribution change complicately from 0.2 to 0.5 m across the length. The maximum vluae of tensile σ_y is about 50 MPa and lies in the left of profile (Fig. 1). It is obviously the σ_z

distribution along A and B, F and H is symmetry due to the balance effect of deformation. The slower cooling rate of B leads to less deformation compared with A andfasttemperature decrement results in the larger compressed stress -55 MPa in the right of profile. Furtheremore, there are resuidal stress σ_x and σ_y in the profile after quenching but the free deformation in the extrusion direction results in σ_z decreasing to zero.

The non-uniform deformation as a result of different thickness and cooling boundary conditions has important effect on the distortion and fracture. Different intial cooling rate and mixed cooling methods were used to online quenching according to the thickness of profile in order to improve distortion and deformation. Based on the idea of cold rolling with tension, the head of profile was streched in the extrusion direction during online quenching.

Fig. 9 shows the displacement and equivalent stress with external stretching force. The external tension is realized by applying the force to the cross-section nodes of head of profile. In the paper, the nodal force is set to 50, 100 and 120 N. It can be seen that every component displacement is reduced significantly with nodal force 100 N compared with no external tension. Furthermore, the equivalent stress is also reduced from 57.2 to 52.7 MPa with nodal force 50 N. The equivalent stress and displacement are reduced significantly with the external stretching force. However, the displacements of these typical points increase greatly in an opposite direction and the maximum X-component displacement of point A and C is about 60 mm when the nodal force is 120 N. It is also found from the Z-component displacement the profile is stretched compared with the initial size but the displacement should be less than zero because of cold shrinkage. Moreover, the equivalent stress increase up to 75 MPa with the nodal force 120 N compared with that of 50 N. Therefore, the suitable external tension is benefit to improve the distortion and avoid the fracture.

4. Conclusions

1. The temperature and displacement of a plate during quenching is studied by numerical simulation and experiments. The calculated temperature and displacement are in good agreement with the measured value and the developed FE model on the basis of the ANSYS is reliable.

2. The temperature decreases significantly at initial water cooling stage and then becomes slower. After quenching, the maximum temperature of head of the profile is less than about 80℃, which the cooling rate is satisfied with the requirements. More thickness results in temperature decreasing more slowly and the temperature difference across the section increases up to a maximum value and then decreases to a final value.

3. Non-uniform deformation is more obviously with the increment of quenching length. The maximum x-component and y-component displacement is about 10mm and 3mm, respectively, one meter length of quenching. More complex cross-section and thickness difference result in larger tensile stress.

4. The displacement and equivalent stress is reduced significantly with external stretching force during online quenching process. Lower stretching force has less

effect on the improvement of distortion but larger load will result in opposite plastic deformation and fracture.

Acknowledgements

References

1. **Panigrahi, S.K.; Jayaganthan, R.A.** 2008. Study on the mechanical properties of cryorolled Al-Mg-Si alloy, Materials Science and Engineering A, 480(1-2): 299-305.
   http://dx.doi.org/10.5755/j01.mech.20.6.9157.
2. **Bikass, S.; Andersson, B.; Pilipenko, A. et al.** 2012. Simulation of initial cooling rate effect on the extrudate distortion in the aluminum extrusion process, Applied Thermal Engineering 40: 326-336.
   http://dx.doi.org/10.1016/j.applthermaleng.2012.02.012.
3. **Gbenebor, O.P.; Abdulwahab, M.; Fayomi, O.S.I. et al.** 2012. Influence of inoculant addition and cooling medium on the mechanical properties of AA6063-type Al-Mg-Si alloy, Chalcogenide Letters 9(5): 201-211.
4. **Li, H.Y.; Zeng, C.T.; Han, M.S. et al.** 2013. Time-temperature-property curves for quench sensitivity of 6063 aluminum alloy, Transactions of Nonferrous Metals Society of China 23(1): 38-45.
   http://dx.doi.org/10.1016/S1003-6326(13)62426-7.
5. **Sheppard, T.** 1988. Press quenching of aluminum, Materials Science and Technology 4(7): 635-643.
   http://dx.doi.org/10.1179/mst.1988.4.7.635.
6. **Bikass, S.; Andersson, B.; Pilipenko, A. et al.** 2012. Simulation of the distortion mechanisms due to non-uniform cooling in the aluminum extrusion process, International Journal of Thermal Sciences 52: 50-58.
   http://dx.doi.org/10.1016/j.ijthermalsci.2011.06.002.
7. **Qian, Z.Y.; Chumbley, S.; Johnson E.** 2011. The effect of specimen dimension on residual stress relaxation of carburized and quenched steels, Materials Science and Engineering A, 529: 246-252.
   http://dx.doi.org/10.1016/j.msea.2011.09.024.
8. **Yang, X.W.; Zhu, J.C.; Nong, Z.S. et al.** 2013. FEM Simulation of quenching process in A357 aluminum alloy cylindrical bars and reduction of quench residual stress through cold stretching process, Computational Materials Science 69: 396-413.
   http://dx.doi.org/10.1016/j.commatsci.2012.11.024.
9. **Li, L.X.; Hu, L.Z.; Liu, Z.W. et al.** 2013. Simulation study of the quenching process and parameter improvement of aluminum extrusion, Journal of Hunan University (Natural Sciences) 40(2): 71-76.
10. **Holzapfel, H.; Schulze, V.; Vohringer, O.; Macherauch, E.** 1998. Residual stress relaxation in an AISI 4140 steel due to quasistatic and cyclic loading at higher temperatures, Materials Science and Engineering A, 248(1): 9-18.
    http://dx.doi.org/10.1016/S0921-5093(98)00522-X.
11. **Qian, Z.Y.; Chumbley, S.; Karakulak, T.; Johnson, E.** 2013. The residual stress relaxation behavior of weldments during cyclic loading, Metallurgical and Materials Transactions A, 44(7): 3147-3156.
    http://dx.doi.org/10.1007/s11661-013-1688-9.
12. **Zhuang, W.Z.; Halford, G.R.,** 2001. Investigation of residual stress relaxation under cyclic load, International Journal of Fatigue 23(1): 31-37.
    http://dx.doi.org/10.1016/S0142-1123(01)00132-3
13. **Nallathambi, A.K.; Kaymak, Y.; Specht, E.; Bertram, A.** 2009. Optimum strategies to reduce residual stresses and distortion during the metal quenching process, Journal of ASTM International 6(4): 411-435.
14. **Pietzsch, R.; Brozoza, M.; Kaymak, Y. et al.** 2007. Simulation of the distortion of long steel profiles during cooling, Journal of Applied Mechanics 74(3): 427-437.
    http://dx.doi.org/10.1115/1.2338050.
15. **Zabaras, N.; Mukherjee, S.; Arthur, W.R.** 1987. A numerical and experimental study of quenching of circular cylinders, Journal of thermal stresses 10(3): 177-191.
16. **Carlone, P.; Palazzo, G.S.; Pasquino, R.** 2010. Finite element analysis of the quenching process: temperature field and solid-solid phase change, Computational and Applied Mathematics 59(1): 585-594.
    http://dx.doi.org/10.1016/j.camwa.2009.06.006.
17. **Carlone, P.; Palazzo, G.S.** 2011. Development and validation of a thermo-mechanical finite element model of the steel quenching process including solid-solid phase change, International Applied Mechanics 46(8): 955-971.
    http://dx.doi.org/10.1007/s10778-011-0386-9.
18. **Caspi, S.; Chiesa, L.; Ferracin, P. et al.** 2003. Calculating quench propagation with ANSYS, IEEE Transactions on Applied Superconductivity 13(2): 1714-1717.
    http://dx.doi.org/10.1109/TASC.2003.812867.
19. **Liu, L.G.; Liao, B.; Li, D.; et al.** 2011. Thermal-elastic-plastic simulation of internal stress fields of quenched steel 40Cr cylindrical specimens by FEM, Materials and Manufacturing Processes 26(5): 732-739.
    http://dx.doi.org/10.1080/10426910903367428.
20. **Li, N.K.; Ling, G.; Nie, B.; et al.** 2012. Aluminum Alloy and Heat Treatment Technology, Beijing: Metallurgical Industry Press, 516p.
21. **Mei, R.B.; Li, C.S.; Liu, X.H. et al.** 2010. Analysis of strip temperature in hot rolling process by finite element method, Journal of Iron and Steel Research (International) 17(2): 17-21.
22. **Ji, Z.L.; Li, Y.H.; Li., Y.Z.** 2013. Thermo-plastic finite element analysis for metal honeycomb structure, Thermal Science 17(5): 1285-1291.
    http://dx.doi.org/10.2298/TSCI1305285J.

R.B. Mei, L. Bao, C.S. Li, J.K. Wang, X.H. Liu

FE ANALYSIS OF 6063 ALUMINIUM PROFILES
WITH COMPLEX CROSS-SECTION DURING ONLINE
QUENCHING PROCESSES

S u m m a r y

Thermal-elastic-plastic finite element (FE) theory and solution of thermal-structural coupled field were investigated on the basis of commercial software ANSYS. The FE model used to solve the transient air and water cooling

processes of extrusion profiles was built through developed programs on the basis of ANSYS. The calculated temperature and displacement of a plate during water cooling are in good agreement with the measured value and the FE model is reliable. Consequently, the temperature, displacement and equivalent stress of a complex cross-section profile from a plant during online quenching process were investigated. Thickness and boundary conditions difference leads to the temperature difference across the section increases up to about 120°C firstly and then decrease to less than 40°C. For the complex cross-section profile, the non-uniform deformation is more obviously and the larger thermal stress is the main reason of plastic deformation, fracture generation and occurrence of higher residual stress. A method used external stretching force to improve the distortion was also proposed in quenching processes and the displacement and equivalent stress is reduced significantly through external stretching force. However, larger external stretching force perhaps results in more serious distortion and fracture.